

LETTER TO THE EDITOR

Evolution and Magnitudes of Candidate Planet Nine

Esther F. Linder and Christoph Mordasini

Physikalisches Institut, University of Bern, Sidlerstrasse 5, 3012 Bern, Switzerland

Received 19.02.2016 / Accepted —

ABSTRACT

Context. Given the recently renewed interest in a possible additional major body in the outer Solar System, the thermodynamic evolution of such an object was studied, assuming that it is a smaller version of Uranus and Neptune.

Aims. We have modeled the temporal evolution of the radius, temperature, intrinsic luminosity, and the black body spectrum of distant ice giant planets. The aim is also to provide estimates of the magnitudes in different bands to assess the object's detectability.

Methods. Simulations of the cooling and contraction were conducted for ice giants with masses of 5, 10, 20, and $50 M_{\oplus}$ containing 10, 14, 21, and 37 % H/He in mass that are located at 280, 700, and 1120 AU from the Sun. The core composition was varied from purely rocky to purely icy as well as 50% rock and 50% ice. The atmospheric opacity was set to 1, 50, and 100 times solar metallicity.

Results. We find for the nominal $10 M_{\oplus}$ planet at 700 AU at the current age of the Solar System an effective temperature of 47 K, much more than the equilibrium temperature of about 10 K, a radius of $3.7 R_{\oplus}$, and an intrinsic luminosity of $0.006 L_{\odot}$. It has estimated apparent magnitudes of Johnson V, R, I, L, N, Q of 21.7, 21.2, 20.8, 20.1, 19.7, and 11.4, and WISE W1-W4 magnitudes of 20.1, 20.0, 19.5, and 10.4. The Q and W4 band and other observation longward of about $13 \mu\text{m}$ pick up the intrinsic flux.

Conclusions. If candidate Planet 9 has a significant H/He layer and an efficient energy transport in the interior, then its luminosity is dominated by the intrinsic contribution, making it a self-luminous planet. At a likely position on its orbit near the aphelion, we estimate for a mass of 5, 10, 20, and $50 M_{\oplus}$ a V magnitude from the reflected light of 24.2, 23.7, 23.2, and 22.5 and a Q magnitude from the intrinsic radiation of 15.6, 12.4, 9.8, 6.2. The latter would probably have been detected by past surveys.

Key words. Planets and satellites: detection – Planets and satellites: physical evolution – Oort Cloud – Kuiper belt: general

1. Introduction

The presence of another major body in the Solar System would be of highest interest for planet formation and evolution theory. Based on the observed peculiar clustering of the orbits of trans-Neptunian objects (Brown et al. 2004; Trujillo & Sheppard 2014) and after analyzing several earlier hypotheses (de la Fuente Marcos & de la Fuente Marcos 2014; Iorio 2014; Madigan & McCourt 2016), Batygin & Brown (2016) have recently proposed that a $\sim 10 M_{\oplus}$ planet could be present in the outer Solar System at a distance of several hundred AU from the Sun. Following the historical example of Neptune, the next step would be the observational discovery of the object. Depending on its specific properties, because of faintness, slow motion on the sky, and confusion with galactic background stars, the object could in principle have evaded detection up to now. In this letter, we present predictions for the physical properties of a planet like the one proposed, which is important for its detectability. Given its most likely mass and the extrasolar planetary mass-radius relation (e.g., Gettel et al. 2016), we assume that candidate Planet 9 has the same basic structure as Uranus and Neptune. As already speculated by Batygin & Brown (2016), it could be an ejected failed giant planet core. Planets of this type form frequently in planet formation simulations based on the core accretion theory (Mordasini et al. 2009) and can get scattered to large distances by giant planets (Bromley & Kenyon 2011).

2. Evolution Model

Our planet evolution model (Mordasini et al. 2012) calculates the thermodynamic evolution of planetary parameters (like the

luminosity or planetary radius) over time for a wide range of initial conditions. The planet's structure is simplified by assuming a central core consisting of iron which is wrapped in a silicate mantel followed by a possible water ice layer and finally a H/He envelope. For the luminosity, the contributions of the contraction and cooling of the gaseous envelope and of the solid core are included, as well as radiogenic heating. The interior is assumed to be adiabatic. The atmospheric model is gray and modeled with the condensate-free opacities of Freedman et al. (2014). Stellar irradiation is included via the Baraffe et al. (2015) tracks. The simulations start at 10 Myr at a prespecified initial luminosity, but its value is inconsequential for the properties at 4.6 Gyr.

3. Simulations

Based on the nominal scenario in Batygin & Brown (2016), we started our study with a planet of $10 M_{\oplus}$ at a semimajor axis of 700 AU. Given the typical core-to-envelope mass ratio found in planet formation simulations (Mordasini et al. 2014), we assumed the core and envelope masses to be 8.6 and $1.4 M_{\oplus}$, respectively. This is compatible with the estimated H/He mass fractions of Uranus (12-15%) and Neptune (16-19%, Guillot & Gautier 2014). The initial luminosity was also taken from the formation simulations and set to $1.41 L_{\odot}$, comparable to Fortney et al. (2011). The core composition is 50% water ice (referred to as „ice“ in the following), 33.3% silicates, and 16.7% iron (referred to as „rock“ in the following). The atmosphere is assumed to be gray, with an opacity corresponding to 50 times solar enrichment. This first simulation will be called the „nominal case“ in the following. To calculate magnitudes, a black body spectrum for the planet, tabulated values for the flux of Vega

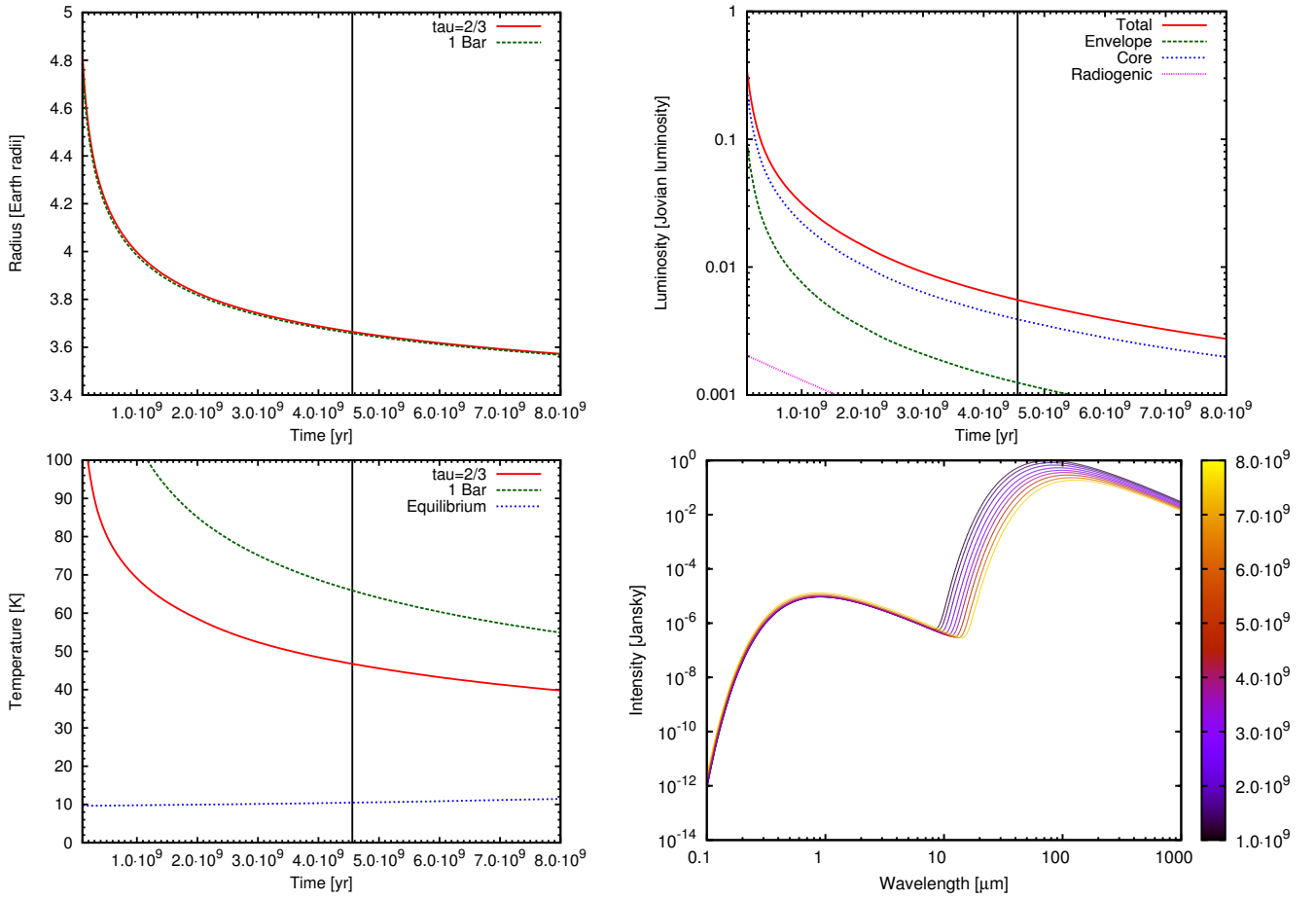


Fig. 1: Temporal evolution of fundamental properties of a $10 M_{\oplus}$ planet at 700 AU with a $1.4 M_{\oplus}$ H/He envelope, a core consisting of 50% ice and 50% rock, and a 50 times solar atmospheric opacity. *Top left:* Radius. *Top right:* Intrinsic luminosity. *Bottom left:* Temperature. *Bottom right panel:* Black body spectrum where the age in years is given by the color code.

(Allen & Cox 2000), and simplified rectangular filter transmissions (Traub & Oppenheimer 2010) were used. We calculated the reflected flux from the object assuming it is at full phase. The Bond and geometric albedo were fixed for simplicity to 0.31 and 0.41, Neptune's values (Traub & Oppenheimer 2010).

For non-nominal simulations, the planet's mass was varied, being 5, 20, and $50 M_{\oplus}$ with envelope mass fractions of 10, 21, and 37 % as representative for the aforementioned formation simulations from where we also took the initial luminosities of 0.32, 6.27, and $44.96 L_{\oplus}$, respectively. Also the core composition was varied, assuming a purely rocky and purely icy core. The opacity of the atmosphere, corresponding to 1 and 100 times solar enrichment, roughly the enrichment of carbon in Uranus and Neptune (Guillot & Gautier 2014), was varied as well. To account for the high eccentricity of the object, the semimajor axis was changed to 280 and 1120 AU.

4. Results

4.1. Nominal Simulation

Figure 1 shows the evolution of the radius, luminosity, temperature and black body spectrum for the nominal case. The top left panel shows that the 1 bar radius is today at $3.66 R_{\oplus}$ equal to 23'300 km. The top right panel shows the decrease of the total, envelope, core, and radiogenic luminosity in time. The current

total intrinsic luminosity is $0.006 L_{\oplus}$, with a dominant contribution from the core's thermal cooling. For comparison, Neptune has an intrinsic luminosity of $0.01 L_{\oplus}$ (Guillot & Gautier 2014). As visible in the bottom left panel, the current temperature at $\tau=2/3$ is 47 K. The wavelength of maximum black body emission at a temperature of 47 K follows from Wien's law and is $62 \mu\text{m}$, in the far-IR. This temperature is much more than the equilibrium temperature of about 10 K at 700 AU. The planet's energy budget is thus dominated by the intrinsic flux. For this, the assumption of a fully convective interior is critical. Without efficient energy transport, the planet's intrinsic luminosity could be much smaller, as for Uranus (Nettelmann et al. 2013). The temperature at the 1 bar level is about 66 K, while at the envelope-core boundary around 2100 K are reached. It can also be seen that the equilibrium temperature is slowly rising due to the Sun's evolution. The evolution of the black body spectra is shown in the bottom right panel. The reflected contribution at wavelengths less than $\sim 13 \mu\text{m}$ remains nearly constant whereas the higher and varying intrinsic contribution in the mid and far-IR follows the intrinsic luminosity. Non-gray effects can significantly modulate the actual spectrum (e.g., Traub & Oppenheimer 2010).

4.2. Magnitudes in Various Bands along one Orbit

For an age of 4.56 Gyr, when the luminosity is $0.006 L_{\oplus}$ a simulation with nominal parameters was carried out where the

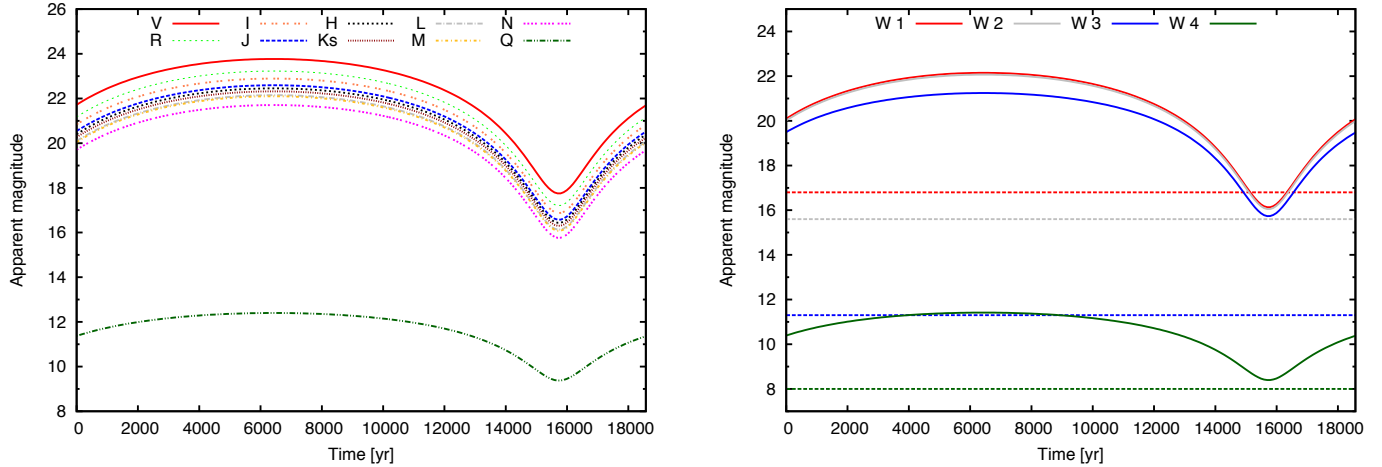


Fig. 2: Present-day apparent magnitudes for the nominal $10 M_{\oplus}$ planet during one orbit around the Sun at $a=700$ AU and $e=0.6$. *Left panel*: Johnson V to Q. *Right panel*: WISE filters, together with $S/N=5$ limits shown by dashed horizontal lines (Luhman 2014).

planet's heliocentric distance varies in time, as found from solving the Kepler equation. The thermal timescale of the atmosphere (outer radiative zone) is on the order of 100 years as found from dividing the atmospheric thermal energy content by the luminosity. This is much less than the orbital timescale, thus the atmosphere should adapt to the varying stellar irradiation without significant thermal inertia. Figure 2 shows the apparent magnitudes for various bands for the nominal case during one orbit around the Sun at a semimajor axis of 700 AU and an eccentricity of 0.6, as proposed by Batygin & Brown (2016). At a distance of 700 AU, the planet has estimated apparent magnitudes of Johnson V, R, I, L, N, Q of 21.7, 21.2, 20.8, 20.1, 19.7, and 11.4. In the Q filter the intrinsic luminosity of the planet is seen. The planet is thus much brighter in the mid and far infrared than in the visual or near infrared. The Wide-Field Infrared Survey Explorer (WISE) magnitudes W1, W2, W3, and W4 are shown in the right panel, being 20.1, 20.0, 19.5, and 10.4 at 700 AU. The magnitudes at other heliocentric distances r are simply found from the $1/r^4$ dependency for the reflected flux, meaning that at perihelion it is 4 mag brighter and 2 mag dimmer at aphelion, while for the intrinsic flux (Q and W4), the $1/r^2$ dependency means that at perihelion it is 2 mag brighter, and at aphelion it is 1 mag dimmer. In the right panel the WISE $S/N=5$ limits of W1=16.8, W2=15.6, W3=11.3, and W4=8.0 (Luhman 2014) are also shown, indicating the possibility to see the object with WISE only close to perihelion with the W1 filter. The actual detection limit of the survey of Luhman (2014) is W2=14.5 given by the ability of detecting an object in multiple epochs.

4.3. Long Term Evolution of the Magnitudes and Non-Nominal Simulations

In Figure 3, apparent magnitudes in the V and Q band are shown for the nominal planet and planets where the mass relative to the nominal case was varied. In general, it can be seen that the objects are brighter in the Q band than in the V band. Since in the V band the reflected light of the Sun can be seen, the objects get slightly brighter with time, mirroring the evolution of the Sun. By contrast, in the Q band, which shows the intrinsic radiation of the planet, the planets get slowly fainter due to cooling.

Impact of the mass. In the figure, besides the nominal $10 M_{\oplus}$ case, the apparent magnitude's evolution is shown for planets of 5, 20, and $50 M_{\oplus}$. These planets have a present-day radius

of 2.92, 4.62, and $6.32 R_{\oplus}$, an intrinsic luminosity of 0.0018, 0.016, and $0.078 L_{\oplus}$, and an effective temperature of 39.8, 54.4, and 68.9 K, respectively. The V band magnitudes are 22.2, 21.2, and 20.5 mag, and the Q band magnitudes are 14.6, 8.8, and 5.3 mag, respectively.

Core composition. The influence on the magnitude from a change in core composition relative to the nominal case is small. For the V band, the planet with a rocky core is the faintest (21.9 mag) while the planet with a purely icy core is the brightest (21.6 mag) owing to a radius that is $0.3 R_{\oplus}$ smaller and larger in respect to the nominal case. In the Q band the planet with the purely icy core is also brighter (11.0 mag) than for a purely rocky core (12.3 mag) now due to the higher heat capacity of water (Baraffe et al. 2008).

Atmospheric opacity. A variation of the opacities corresponding to 1, 50, and 100 solar enrichment has a very small effect on the V and Q band magnitudes for the $10 M_{\oplus}$ planet (differences of less than 0.2 mag).

Orbital distance. We simulated the evolution of the $10 M_{\oplus}$ planet at a fixed distance of 280 and 1120 AU (the estimated perihelion and aphelion distances of candidate Planet 9) instead of 700 AU. The resulting present-day physical properties of the planet are virtually unchanged, showing that the interior's evolution proceeds as if the planet was in isolation. This means that the change of the planet's magnitude along its orbit is simply due to the change in its heliocentric distance. For example, the V and Q magnitudes at aphelion are thus 2.04 and 1.02 mag fainter than at 700 AU.

5. Discussion and Conclusion

Motivated by the recent suggestion by Batygin & Brown (2016) regarding a possible additional planet in the Solar System, the evolution in radius, luminosity, temperature, and black body spectrum of a $10 M_{\oplus}$ planet at 700 AU was studied, assuming that it is a smaller version of Uranus and Neptune. It was found that today the radius of such an object is about $3.66 R_{\oplus}$. The intrinsic luminosity of the planet is today about $0.006 L_{\oplus}$ with the biggest contribution coming from the thermal cooling of the core. The effective temperature of the object is with 47 K much higher than its equilibrium temperature of 10 K, meaning that the planet's emission is dominated by its internal cooling and contraction. Its intrinsic power is about 1000 times bigger than

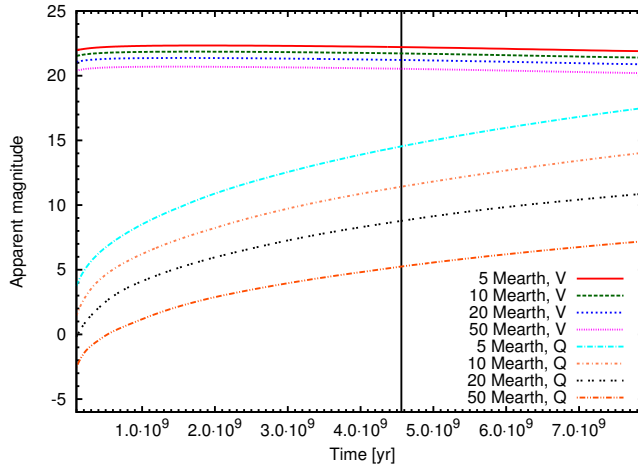


Fig. 3: Long-term evolution of the apparent magnitudes in V and Q for the nominal case and planets with masses of 5, 10, 20 and $50 M_{\oplus}$.

its absorbed power, making it a self-luminous planet. For comparison, Jupiter's intrinsic power is around half as high as its absorbed power (Guillot & Gautier 2014). This dominance can also be seen in the evolution of the black body spectrum of the planet, where the evolving intrinsic flux is much higher than the reflected flux. It also means that the planet is much brighter in the mid and far-IR than in the visual and near-IR.

The effect on the apparent magnitude of the planet in the V and Q band was studied for a variation in the planet's mass, its semimajor axis, its core composition as well as its atmospheric opacity. For the examined parameter range, the biggest influence on the Q band comes from the planetary mass, whereas the biggest influence on the V band comes from the planet's semimajor axis. This is not surprising, since in the Q band, the intrinsic luminosity of the planet is seen, which is most sensitive to its mass. In contrast, the reflected light is seen in the V band, which is most sensitive to the planets distance from the Sun.

Many surveys in various wavelength domains and with different sensitivities were performed in the past. For example Trujillo & Brown (2003) observed 12% of the sky near the invariable plane in the R band with a sensitivity limit of 20.7 mag. Candidate Planet 9 is however most of the time fainter than 22 mag in the R band (Fig. 2), and additionally, it is assumed to have an inclination of $i = 30^\circ$ (Batygin & Brown 2016). Therefore, there was only a small possibility for Trujillo & Brown (2003) to detect candidate Planet 9. Another study was done by Elliot et al. (2005) who observed the sky within 6° of the ecliptic with a VR filter down to a limit of 22.5 mag. Also in this survey, the probability to detect candidate Planet 9 was low because of the small overlap of the planet's orbit and the surveyed fields. The same is the case for a study by Larsen et al. (2007), who observed the sky in the V filter down to a magnitude of 21 within 10° of the ecliptic. For comparison, at aphelion at 1120 AU, we find V magnitudes of 24.2, 23.7, 23.2, and 22.5 for masses of 5, 10, 20, and $50 M_{\oplus}$ for candidate Planet 9. Schwamb et al. (2010) studied the sky within 30° of the ecliptic, excluding fields less than 15° from the galactic plane. They had a relatively good coverage of candidate Planet 9's orbit, except when it was near 13 h RA or in front of the Milky Way which corresponds to the likely aphelion position of candidate Planet 9 (Brown & Batygin 2016). The survey was done in the R band down to a luminosity of 21.3 mag, whereas we find R magnitudes exceeding 22 mag

near aphelion even for a $50 M_{\oplus}$ version of Planet 9. Sheppard et al. (2011) surveyed the southern sky and galactic plane down to -25° in the R filter down to a depth of 21.6 mag. The observed fields show a relatively good coverage of candidate Planet 9's orbit and they also came closest to the requested brightness, but still did not reach it. Additionally, their astrometric precision goes to $0.5''/\text{hr}$, whereas candidate Planet 9 rather has a movement of around $0.3''/\text{hr}$ (Brown & Batygin 2016). A search in the IR domain was performed by Luhman (2014), who inspected the WISE data for a distant companion to the Sun (see also Schneider et al. 2016). The WISE satellite mapped the whole sky twice and started mapping it a third time. The detection limits of WISE together with our calculated apparent magnitudes for the nominal case were shown in Fig. 2. The possibility for WISE to detect a $10 M_{\oplus}$ Planet 9 is small because of the brightness limits. However, if the planet should be more massive, a detection becomes more probable, at least from the brightness limit alone. Especially the $50 M_{\oplus}$ mass planet would have been visible in W4 during its entire orbit, putting an interesting upper mass limit for the planet. In summary, the current null result seems compatible with nominal candidate Planet 9 properties especially if it is at aphelion. In contrast, future telescopes like the Large Synoptic Survey Telescope with a sensitivity down to R=26 mag (Luhman 2014) or dedicated surveys should be able to find or rule out candidate Planet 9 which is an exciting perspective.

Acknowledgements. We thank M. R. Meyer, Y. Alibert, K. Heng, S. Udry, K. Zihlmann, and W. Benz for valuable inputs to the discussion. E.F.L. and C.M. acknowledge the support from the Swiss National Science Foundation under grant BSSGI0.155816 “PlanetsInTime”. Parts of this work have been carried out within the frame of the National Center for Competence in Research PlanetS supported by the SNSF.

References

- Allen, C. & Cox, A. 2000, Allen's Astrophysical Quantities (Springer)
- Baraffe, I., Chabrier, G., & Barman, T. S. 2008, A&A, 482, 315
- Baraffe, I., Homeier, D., Allard, F., & Chabrier, G. 2015, A&A, 577, A42
- Batygin, K. & Brown, M. E. 2016, AJ, 151, 22
- Bromley, B. C. & Kenyon, S. J. 2011, ApJ, 731, 101
- Brown, M. E. & Batygin, K. 2016, <http://www.findplanetnine.com>
- Brown, M. E., Trujillo, C., & Rabinowitz, D. 2004, ApJ, 617, 645
- de la Fuente Marcos, C. & de la Fuente Marcos, R. 2014, MNRAS, 443, L59
- Elliot, J. L., Kern, S. D., Clancy, K. B., et al. 2005, AJ, 129, 1117
- Fortney, J. J., Ikoma, M., Nettelmann, N., Guillot, T., & Marley, M. S. 2011, ApJ, 729, 32
- Freeman, R. S., Lustig-Yaeger, J., Fortney, J. J., et al. 2014, ApJS, 214, 25
- Gettel, S., Charbonneau, D., Dressing, C. D., et al. 2016, ApJ, 816, 95
- Guillot, T. & Gautier, D. 2014, Treatise on Geophysics 2nd Edition (Eds. T. Spohn, G. Schubert)
- Iorio, L. 2014, MNRAS, 444, L78
- Larsen, J. A., Roe, E. S., Albert, C. E., et al. 2007, AJ, 133, 1247
- Luhman, K. L. 2014, ApJ, 781, 4
- Madigan, A.-M. & McCourt, M. 2016, MNRAS, 457, L89
- Mordasini, C., Alibert, Y., & Benz, W. 2009, A&A, 501, 1139
- Mordasini, C., Alibert, Y., Klahr, H., & Henning, T. 2012, A&A, 547, A111
- Mordasini, C., Klahr, H., Alibert, Y., Miller, N., & Henning, T. 2014, A&A, 566, A141
- Nettelmann, N., Helled, R., Fortney, J. J., & Redmer, R. 2013, Planet. Space Sci., 77, 143
- Schneider, A. C., Greco, J., Cushing, M. C., et al. 2016, ApJ, 817, 112
- Schwamb, M. E., Brown, M. E., Rabinowitz, D. L., & Ragozzine, D. 2010, ApJ, 720, 1691
- Sheppard, S. S., Udalski, A., Trujillo, C., et al. 2011, AJ, 142, 98
- Traub, W. A. & Oppenheimer, B. R. 2010, Direct Imaging of Exoplanets, ed. S. Seager (Tucson, AZ: University of Arizona Press), 111–156
- Trujillo, C. A. & Brown, M. E. 2003, Earth Moon and Planets, 92, 99
- Trujillo, C. A. & Sheppard, S. S. 2014, Nature, 507, 471